Pergamon

Int. J. Solids Structures Vol. 33, No. 16, pp. 2357–2376, 1996

0020-7683/96 $15.00 + .00

0020-7683(95)00157-3

A SIMPLE NUMERICAL MODEL FOR ANALYSIS OF PROPPED EMBEDDED RETAINING WALLS

H. H. VAZIRI
Department of Civil Engineering, Technical University of Nova Scotia, P.O. Box 1000, Halifax, N.S., Canada B3J 2X4

(*Received* 9 *September* 1994; *in revised form* 12 *July* 1995)

Abstract—A simple, efficient and practical numerical model is described for analysis of cantilevered and strutted flexible retaining walls. The model accommodates a variety of features that affect the performance of retaining walls in the field such as application and removal of struts, application of surcharge, changes in the water table, changes in the soil properties and simulation of staged excavations. Unlike conventional finite element and finite difference models that require a considerable effort and knowledge to prepare the input data, the proposed model requires only a few lines of data to define the problem and control the analysis. The computational results include bending moment, shear force and deflection of the wall, strut loads and lateral stresses in the soil at any stage of the analysis. The model can be used effectively to perform a broad suite of parametric studies at the design stage and also as a reliable tool for predicting performance. To demonstrate the latter, the model is applied to analyze several problems involving different wall types in stiff and soft soils. Despite the implicit idealizations in the formulation of the model, such as a linear variation of soil stiffness with depth, the model is shown to provide results that are acceptable for design purposes and of the same quality as those obtained from conventional finite element models.

INTRODUCTION

Design of earth-retaining structures requires knowledge of the earth and water pressures that will be exerted on them. The conventional approach for determination of earth pressures uses the classical Rankine method where the retaining wall is assumed to be rigid and to move as a unit and where the soil pressure on either side of the wall is assumed to be at its limit state. Design predictions based on Rankine's theory work quite well in the case of gravity walls which have sufficient rigidity to avoid bending deformations but which can move as a unit. However, despite the fact that Rankine's method provides simple and generally acceptable means for estimating earth pressures, the inherent assumptions ignore the true effects of soil-structure interaction and the processes of construction of the system. These limitations become serious under certain practical conditions where flexible systems are employed to retain the earth. The wall and struts flexibility characteristics affect the mode and magnitude of deformations and result in a corresponding complex distribution of earth pressures that may be quite different than those obtained from the idealized Rankine-based theory.

To investigate the behaviour of flexible retaining walls at working stresses and to predict wall and ground movements has generally involved the use of non linear finite element methods (e.g., Whittle *et al.*, 1993). However, for routine analysis within the design office finite element methods tend to be expensive and complex and therefore susceptible to error. Consequently a simpler analysis is desirable. Such simple analyses traditionally have been performed using subgrade reaction models (also known as Winkler's model). Unfortunately, the rationale behind such models is fundamentally weak as they require specification of equivalent spring stiffnesses to simulate the response of soils. Representation of soil stress-strain characteristics via a set of linear elastic springs cannot be accomplished in a reliable and consistent fashion.

In order to overcome the disadvantages of using a subgrade reaction method the soil can be modelled as an elastic continuum whose stiffness can be determined by Young's modulus. A method based on such an assumption is described in Vaziri and Troughton

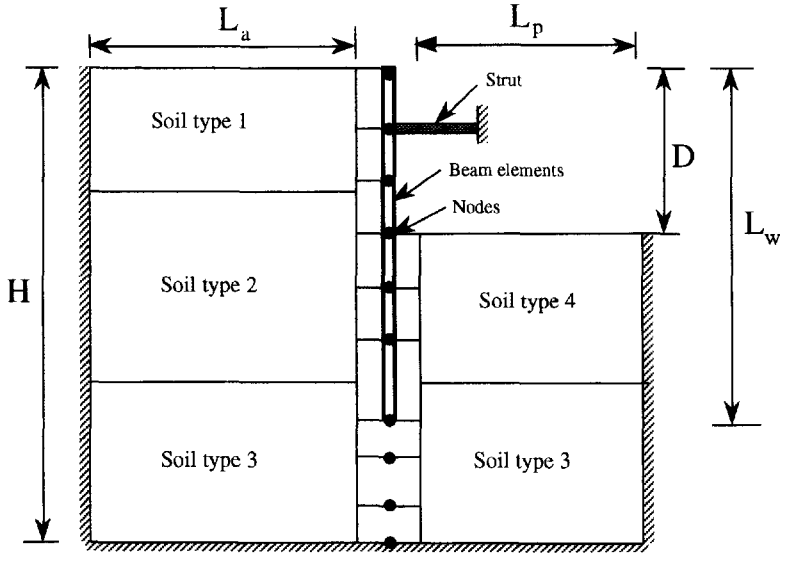

Fig. 1. Connection of the soil mass and struts to the wall and the general geometry.

(1992) wherein the integrated form of Mindlin's equations (Vaziri *et al.*, 1982) is employed to represent the soil as an elastic block having a constant Young's modulus. Although this method provides a very efficient means of performing three dimensional analysis, it does so at the expense of assuming a constant stiffness with depth. The method presented herein removes this limitation by allowing for the generally observed increase of Young's modulus with depth. The methodology used to incorporate varying stiffness with depth follows the work proposed by Pappin *et al.* (1985) wherein soil stiffnesses are modelled using pre-calculated flexibility matrices obtained from finite element computations for elastic soil blocks. Assumptions and formulations used in the development of the proposed numerical model for the analysis of flexible retaining structures and its application to several field projects are covered in this paper.

GENERAL DESCRIPTION OF THE MODEL

The proposed model is designed to perform stability analysis and to calculate deformation, bending moment and shear force in the wall and forces in any struts resulting from excavation, changes in water pressure or application of surcharge. The model has direct application in constructions involving driven sheetpiles, bored reinforced concrete piles or trench excavated concrete diaphragm walls.

The general problem is a structure embedded within the soil mass as shown in Fig. 1. The symbols shown in Fig. 1 denote the following: D = excavation depth, H = depth to the rigid base, L_w = wall height, L_a and L_p = distance to rigid boundaries on the active and passive sides. The wall is modelled as a series of elastic beam elements joined at the nodes. The lowest node is either the base of the wall or at a prescribed rigid base in the ground beneath the wall. The soil to each side of the wall is connected at the nodes as shown on the figure. Only horizontal forces can be transmitted between the soil and the nodes and these forces are directly related to the earth pressures. Struts or anchors are modelled as forces and spring stiffnesses connected to the appropriate nodes.

The soil mass can be represented as a layered medium on either side of the wall and characterized by the following parameters:

—unit weight, γ;
—coefficient of lateral earth pressure at rest, $K_0 = \sigma'_h/\sigma'_v$ where σ'_h and σ'_v are the effective horizontal and vertical stress, respectively;

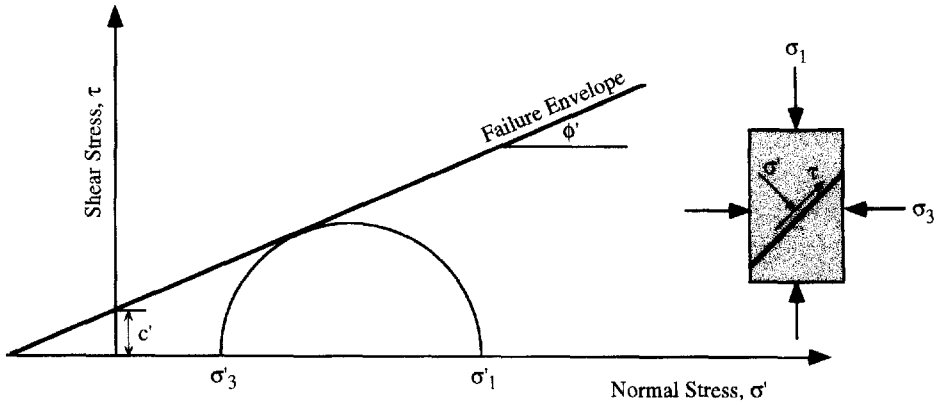

Fig. 2. Representation of strength parameters based on Mohr-Coulomb failure envelope.

—coefficient of active earth pressure, $K_a = (1-\sin\phi')/(1+\sin\phi')$ where ϕ' represents angle of internal friction of the soil and is the slope of the Mohr-Coulomb failure envelope on a shear stress, τ, vs normal effective stress, σ', plot (see Fig. 2);
—coefficient of active earth pressure, $K_p = (1+\sin\phi')/(1-\sin\phi')$;
—the slope of stress path to active failure, K_{ra}, and passive failure, K_{rp}, from the initial stress condition, K_0, as shown in Fig. 3;
—cohesion intercept, c' (see Fig. 2), or undrained shear strength, c_u, if undrained analysis is to be performed;
—Poisson's ratio, v;
—Young's modulus, E.

The behaviour of the retaining wall is described by its Young's modulus, E, multiplied by its second moment of area, I. The struts, which can be prestressed and installed at an incline, are simulated by linear springs and their stiffnesses are defined in terms of spring constants. At any stage of the analysis the following operations can be performed:

—the soil properties (including elastic moduli) can be changed explicitly;
—water pressure on either side of the wall can be changed;
—struts can be inserted and removed (these can be prestressed or inclined);
—surcharges of any dimension at any specified depth can be placed or removed;
—the position of the left- and right-hand fixed boundaries can be changed.

In the following sections, the formulations used to model the soil and structural systems are presented followed by the methodology employed to perform the analysis.

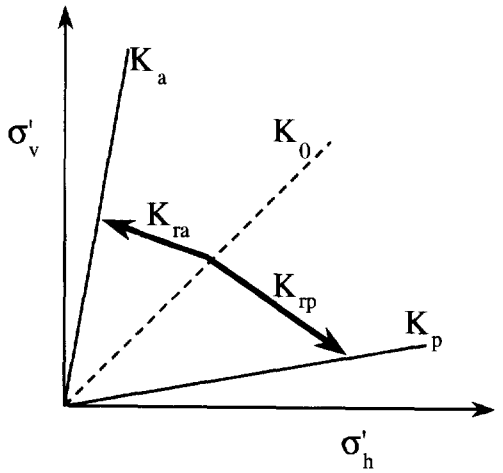

Fig. 3. Specifying direction of stress paths to failure.

Failure

Assuming no adhesion between the wall and the soil, the limiting earth pressures are:

$$\sigma'_{ha} = K_a\sigma'_i - 2c'\sqrt{K_a} \tag{1}$$

$$\sigma'_{hp} = K_p\sigma'_i + 2c'\sqrt{K_p} \tag{2}$$

where σ'_{ha} and σ'_{hp} are the minimum (active) and maximum (passive) lateral effective stresses.

Stiffness

Following the work of Pappin *et al.* (1985), the method adopted in this study obtains stiffness matrices by inverting flexibility matrices derived from a combination of pre-calculated flexibility matrices. These matrices have been calculated using plane strain finite element computations for two different elastic blocks, one with uniform Young's modulus with depth and the other with Young's modulus increasing linearly with depth from zero at the surface. These flexibility matrices define the magnitude of the horizontal displacements at all the nodes on the vertical free surface due to a unit load applied at any one node. The flexibility matrices from the two cases are combined proportionally to cover any situation in which stiffness increases linearly with depth, whatever the value at the free surface. The finite element flexibility matrix is then used to generate an equivalent flexibility matrix compatible with the node spacing used to represent the wall. This manipulation is achieved by scaling the finite element mesh to match the height of the elastic soil block and then linearly combining the flexibility terms to produce the desired matrix.

Linear variation of stiffness with depth can often oversimplify the design profile and therefore an approximate method of adjusting the matrices to accommodate non-linear variations of soil stiffness has been adopted. This method calculates a best fit linear Young's modulus profile E_z^* to represent the actual variation E_z as shown in Fig. 4. The flexibility matrix [**F***] corresponding to the linear approximation can then be derived from the pre-calculated matrices as described above. In order to adjust this matrix to obtain the flexibility matrix [**F**] corresponding to the actual variation of Young's modulus each term in row i or

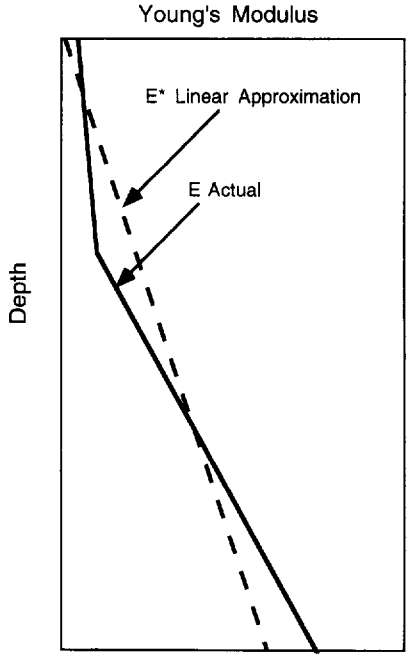

Fig. 4. Linear approximation used to represent nonlinear variation of soil modulus.

[**F***] is multiplied by a coefficient λ_i. To maintain symmetry, terms F_{ij}^* and F_{ji}^* are both multiplied by the same coefficient, chosen as the smaller of λ_i or λ_j.

Pappin *et al.* (1985) considered a number of alternative means of deriving coefficient λ_i and recommended the following

$$\lambda_i = \frac{\int_{z=0}^{H} \frac{E_z^{*2}}{E_z}\left[\frac{\partial \delta_{zi}^*}{\partial z}\right] dz}{\int_{z=0}^{H} E_z^*\left[\frac{\partial \delta_{zi}^*}{\partial z}\right] dz} \tag{3}$$

where δ_{zi}^* is the displacement at depth z of the elastic soil block with Young's modulus profile E_z^* due to unit load at node i.

MODELLING OF THE STRUCTURAL COMPONENTS

In this section derivation of the stiffness matrix for the wall and the struts is shown; these stiffness matrices are then combined to develop the overall stiffness matrix of the structural components (Vaziri, 1995).

The wall is modelled as a series of elastic beam elements, the stiffness matrix being derived using conventional methods from slope deflection equations.

The moments [$\mathbf{M}_w$] and horizontal forces [$\mathbf{P}_w$] at the nodes along the wall are represented as

$$[\mathbf{M}_w] = [\mathbf{A}]\{\delta\} + [\mathbf{B}]\{\theta\} \tag{4}$$

$$[\mathbf{P}_w] = [\mathbf{C}]\{\delta\} + [\mathbf{A}]^T\{\theta\} \tag{5}$$

where $\{\delta\}$ and $\{\theta\}$ are the nodal horizontal displacements and rotations and

$$[\mathbf{A}] = \frac{6EI}{l^2}\begin{bmatrix} 1 & -1 \\ 1 & -1 \end{bmatrix}$$

$$[\mathbf{B}] = \frac{2EI}{l}\begin{bmatrix} 2 & 1 \\ 1 & 2 \end{bmatrix}$$

$$[\mathbf{C}] = \frac{12EI}{l^3}\begin{bmatrix} 1 & -1 \\ -1 & 1 \end{bmatrix}$$

where l is the beam length.

Since there are no moments applied to the wall, it can be shown that the wall stiffness matrix [$\mathbf{K}_w$] is

$$[\mathbf{K}_w] = [\mathbf{C}] - [\mathbf{A}]^T[\mathbf{B}]^{-1}[\mathbf{A}] \tag{6}$$

and eqn [5] can be stated as

$$[P_w] = [\mathbf{K}_w]\{\delta\}. \tag{7}$$

Struts are applied at nodes and are characterized with a prestress force F_S and a stiffness K_S in terms of force/unit displacement. To model the effect of a moment being applied to the wall by a strut a lever arm L_S and inclination α_S can also be specified. This feature is mainly used to model the effect of an inclined strut applying the force eccentrically to the wall section.

The force, P_s, and moment, M_s, applied by the strut at a node are given by

$$P_s = F_s \cos\alpha_s + \delta K_s \cos^2\alpha_s + \theta K_s L_s \cos\alpha_s \sin\alpha_s \tag{8}$$

$$M_s = F_s L_s \sin\alpha_s + \delta K_s L_s \cos\alpha_s \sin\alpha_s + \theta K_s L_s^2 \sin^2\alpha_s. \tag{9}$$

In these expressions δ is the horizontal deflection of the node and θ the rotation of the node since the introduction of the strut. For the special case of a strut inclined at 90° to the wall the above reduces to

$$M_s = F_s L_s + \theta K_s L_s^2. \tag{10}$$

These equations can be written in the form of matrices that represent all struts currently acting on the wall as

$$[\mathbf{P}_s] = [\mathbf{F}_s \cos\alpha_s] + [\mathbf{D}]\{\delta\} + [\mathbf{E}]\{\theta\} \tag{11}$$

$$[\mathbf{M}_s] = [F_s L_s \sin\alpha_s] + [\mathbf{E}]\{\delta\} + [\mathbf{G}]\{\theta\} \tag{12}$$

where

$$[\mathbf{D}] = [\mathbf{K}_s \cos^2\alpha_s]$$

$$[\mathbf{E}] = [K_s L_s \cos\alpha_s \sin\alpha_s]$$

$$[\mathbf{G}] = [K_s L_s^2 \sin^2\alpha_s].$$

The matrix representing the prestress force in the struts is denoted by [**H**] and expressed as

$$[\mathbf{H}] = [F_s \cos\alpha_s] + [[\mathbf{A}] + [\mathbf{E}]]^T [[\mathbf{B}] + [\mathbf{G}]]^{-1} [F_s L_s \sin\alpha_s]. \tag{13}$$

The combined stiffness matrix of the wall and the struts, $[\mathbf{K}_{ws}]$, is given by

$$[\mathbf{K}_{ws}] = [\mathbf{C}] + [\mathbf{D}] - [[\mathbf{A}] + [\mathbf{E}]]^T [[\mathbf{B}] + [\mathbf{G}]]^{-1} [[\mathbf{A}] + [\mathbf{E}]]. \tag{14}$$

With the influence of struts, eqn [7] becomes

$$[\mathbf{P}_{ws}] = [\mathbf{H}] + [\mathbf{K}_{ws}]\{\delta\}. \tag{15}$$

MODELLING OF PRESSURE APPLICATION AND REMOVAL

To account for changes in horizontal effective stress resulting from excavation, application of a uniformly distributed load or changes in pore pressure, the method described in Vaziri (1995) is adopted. In the analysis, the change in horizontal strain is assumed to be zero until the wall is released. This implies that regardless of the position of the current state of stress the following holds:

$$\frac{\Delta\sigma'_h}{\Delta\sigma'_v} = \frac{\nu}{1-\nu} \tag{16}$$

For the case where the vertical effective stress is greater than the preconsolidation stress, a normally consolidated state will be assumed wherein the horizontal effective stress is related to the vertical effective stress via $K_0 (= 1 - \sin\phi')$.

For an elastic material the change in horizontal strain, $\Delta\varepsilon_h$, is related to changes in stress as follows:

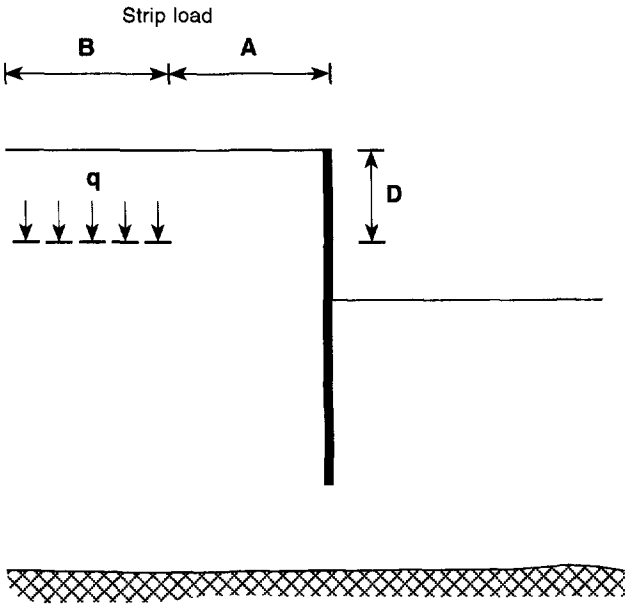

Fig. 5. Surcharge specification by intensity, depth, width and distance from the wall.

$$\Delta\varepsilon_h = \frac{1}{E}[\Delta\sigma'_h - \nu(\Delta\sigma'_h + \Delta\sigma'_v]. \tag{17}$$

Quite frequently application of the load or surcharge tends to be nonuniform in the field; the most common being loads from a strip footing, pad footing or sometimes a point load. The proposed model can simulate surcharge application from a strip load. In this case, as shown in Fig. 5, the surcharge intensity can be specified (q) and its position and dimensions can be characterized by its distance from the wall (A), its width (B) and its depth (D).

The effects of surcharge on the behaviour of the wall are calculated in two steps.

1. Computing the changes in earth pressures acting on the wall before any further displacement occurs.
2. Computing the changes to the active and passive earth pressure limitations. For a uniformly distributed load of an intensity q, they are simply calculated as qK_a and qK_p respectively; for a strip load the effect is more difficult to determine and depends on many factors which are described below.

Since for a strip load the change in stress is quite sensitive to variation of soil stiffness with depth, two extremes are considered: (1) constant E throughout, and (2) E increasing uniformly with depth.

1. *Constant stiffness*

For the case of constant E, Boussinesq's theoretical expressions are used. Boussinesq's solution can be used to develop an expression for the horizontal stress on the wall due to a point load on the surface if two simplifying assumptions are made: (1) the wall does not move, and (2) the wall is perfectly smooth. Under these conditions the stress induced on the wall would be the same as the stress induced in an elastic half-space by two loads of equal magnitude.

2. *Linearly varying stiffness*

For the case where the stiffness increases sharply at a depth less than the width of the surcharge the load will appear to the more flexible soil to act rather like a uniformly distributed load. For the stiffer soil the effect of the surcharge load will still appear as the

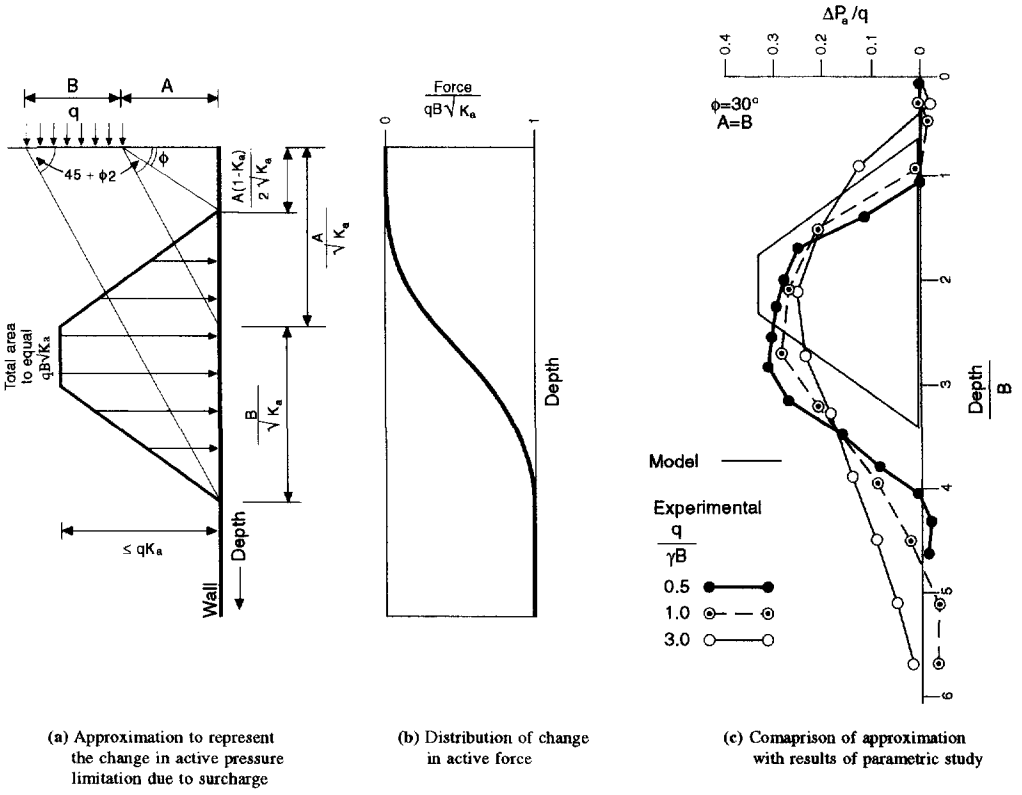

(a) Approximation to represent the change in active pressure limitation due to surcharge

(b) Distribution of change in active force

(c) Comaprison of approximation with results of parametric study

Fig. 6. Effect of surcharge loading on the active pressure limit (Pappin *et al.*, 1985).

Boussinesq pressure. The change of pressure on the wall before further movement can be calculated using

$$[\mathbf{p}] = 2\mu\Delta\sigma_{hB} \tag{18}$$

where $\Delta\sigma_{hB}$ is the change of horizontal stress according to the Boussinesq equations and μ is a correction factor specified by the user. For the constant E case μ should be taken as 1.0. For other cases μ can have a large range of values; for instance if the strip load is wide compared with its distance from the wall and the depth of the deforming soil, an appropriate value for $\mu = \nu/(1-\nu)$.

The effects of a strip surcharge on the active and passive pressure limits can be computed in accordance with Pappin *et al.* (1985) who proposed a relatively simple approximation. Parametric studies were performed using straight line and log spiral shaped failure surfaces for soil that has constant properties with depth. The ranges of variables considered were as follows: ϕ' from 15° to 60°, $q/\gamma B$ from 0.33 to 5 and A/B from 0 to 2. The results showed that the straight line and log spiral methods usually gave very similar results. From purely theoretical considerations the approximation illustrated in Fig. 6a was developed to represent the change in the active pressure limit. This shows the shape of the pressure limit diagram and the criteria for calculation. It should be noted that if the width of the load (B) is small the diagram will become triangular. This distribution of pressure is then used to modify the active pressure limit. Comparison between the theoretical pressure limit change distribution and several curves taken from the parametric study is presented in Fig. 6c. It is seen that the theoretical solution agrees well with the theoretical bearing capacity solutions and is generally conservative.

If K_a varies with depth it is considered conservative to choose a mean value of K_a between any depth z and the level of the surcharge and then impose the criteria that the active force due to the surcharge, down to depth z be equal to the force derived from the

diagram in Fig. 6b. This is then subjected to the further limitation that the pressure never exceeds qK_{az} at any depth, where qK_{az} is the active earth pressure coefficient at depth z.

METHOD OF ANALYSIS

In general the analysis is performed in several steps to depict the main events in the field such as lowering the water table followed by excavation and placement of a strut and further excavation and insertion or removal of other struts etc. At each stage the incremental displacements due to the changes caused by that stage are calculated and added to the existing displacements. The soil stresses, strut forces, wall bending moments and shear forces can then be determined.

At each stage of construction the analysis comprises the following steps:

1. the initial earth pressures and the out of balance nodal forces are calculated assuming no movement of the nodes;
2. stiffness matrices representing the soil on either side of the wall and the wall itself are assembled;
3. these matrices are combined, together with any stiffnesses representing the actions of struts or anchors, to form an overall stiffness matrix;
4. the incremental nodal displacements are calculated from the nodal forces acting on the overall stiffness matrix assuming linear elastic behaviour;
5. the earth pressures at each node are calculated by adding the changes in earth pressure due to the current stage to the initial earth pressures. The derivation of the changes in earth pressure includes multiplying the incremental nodal displacements by the soil stiffness matrices;
6. the earth pressures are compared with soil strength limitation criteria conventionally taken as either the active or passive limits. If any strength criterion is infringed a set of nodal correction forces is calculated. These forces are used to restore earth pressures which are consistent with the strength criteria and also model the consequent plastic deformation within the soil;
7. a new set of nodal forces is calculated by adding the nodal correction forces to those calculated in step 1;
8. steps 4–7 are repeated until convergence is achieved;
9. total nodal displacements, earth pressures, strut forces, wall shear stresses and bending moments are calculated.

APPLICATIONS

To show the performance of the proposed numerical model three cases involving soft and stiff soils and strutted and cantilevered walls have been analyzed. The objective here is not to claim a strict validation of the model as many factors that play a role in the field cannot be truly accounted for. For instance the model cannot directly simulate the effects of parameters that change with time such as the change from undrained to drained behaviour, or the effects of creep (both in soil and the structural components); wall and strutting installation cannot be modelled; and some of the general construction procedures such as excavation in small bays. Also, when comparing computational results with the field measurements considerations must be given to occurrence of any movements prior to installation of monitoring points, location of the monitoring points (distance from the wall and along the wall length) and soil characteristics in the vicinity of the point where measurements are being taken. Despite the complexities associated with accounting for such details, the proceeding analyses show that the model can provide a reasonable quantification of the design requirements and provide a reliable tool for performing parametric studies.

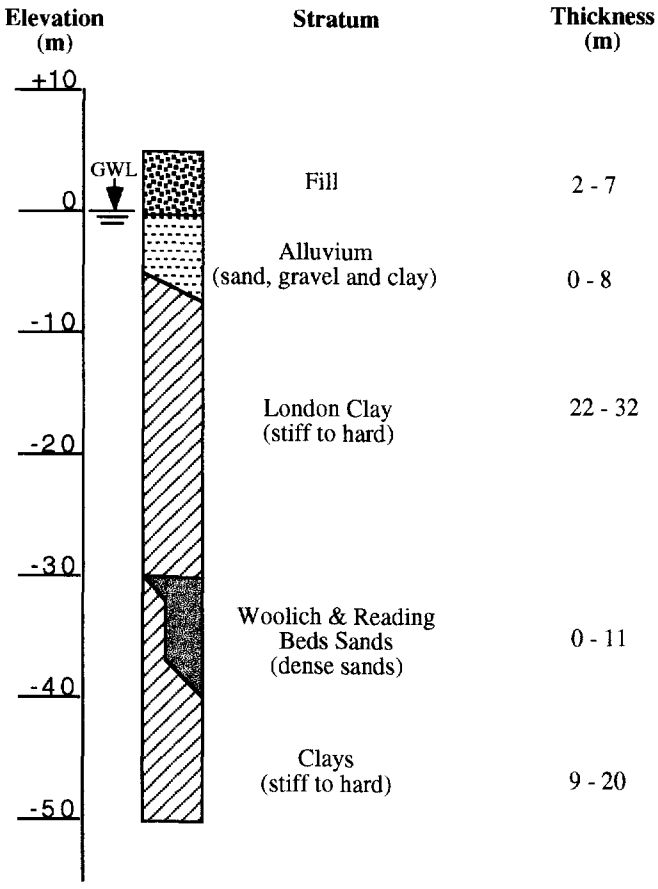

Fig. 7. Simplified geology, Victoria Embankment site (Jardine *et al.*, 1991).

1. *Strutted secant-pile wall in stiff clay*

The geotechnical engineering aspects of a new seven-storey building with four basement levels at Victoria Embankment in London are described in detail by St John *et al.* (1993) and Jardine *et al.* (1991). The excavation extended to a depth of 19 m below ground level, through some fill, alluvium and into a thick deposit of stiff to hard overconsolidated London Clay. A simplified representation of the site stratigraphy is shown in Fig. 7 (Jardine *et al.*, 1991); as it can be observed there were considerable local variations in the thickness of the superficial deposits. Top down construction techniques were used, whereby the permanent perimeter walls were installed using secant piles and, as excavation proceeded, the walls were strutted by the installation of permanent floor structures from the top downwards. The adopted construction sequence is depicted in Fig. 8.

The soil characteristics used to model the problem are shown in Table 1.
A Poisson's ratio of 0.2 was assumed for all layers and the Young's modulus was assumed to vary linearly from the surface in accordance with

$$E' = 3 + 6Z \tag{19}$$

where E' is the elastic modulus in MPa and Z is the depth below ground surface in meters.

Initial lateral stresses were assigned in accordance with the K_0 values shown in Table 1 and a hydrostatic pore water distribution below 3 m depth. On the excavation side, the water table was lowered to the top of the clay layer.

The following dimensions were used in the analysis: wall height, $L_w = 25$ m; depth to the rigid base, $H = 35$ m (i.e., bottom of the Woolich and Reading Beds dense sands); distance to the passive rigid side, $L_p = 18$ m (i.e., half of the excavation width); distance to the active rigid side, $L_a = 25$ m. For the retaining wall a bending stiffness, EI, equal to 50

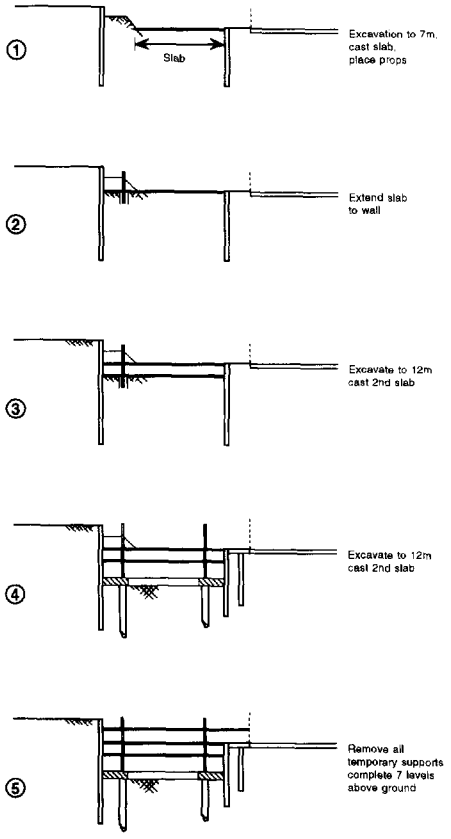

Fig. 8. Sequence used for construction of four basement levels at Victoria Embankment (Jardine *et al.*, 1991).

Table 1. Design parameters to characterize the soil response

Soil type	Consistency	Thickness (m)	γ_{sat} (kN/m^3)	ϕ'	c' (kPa)	K_0	K_a	K_p
Fill	Loose to compact	3.0	17	30	0	0.50	0.33	3.00
Aluvium (sand, gravel and clay)	Compact	2.0	19	33	0	0.46	0.29	3.39
London Clay	Stiff to hard	25.0	19	24	10	3.0	0.42	2.38
Woolich and Reading Beds Sands	Dense	5.0	20	40	0	1.8	0.22	4.50

GN m^2/m was used. In the numerical analysis all the stages shown in Fig. 8 were sequentially modelled with the exception of the berm in Stage 1. The support provided by the berm was modelled using a strut with the stiffness of 40 MN/m/m. The slabs were modelled as struts with an equivalent stiffness of 50 MN/m/m.

The wall movements were monitored by means of inclinometers installed in the secant bored pile retaining wall. Figure 9 shows the comparison between measured and predicted horizontal movements of the retaining wall at one of the locations. Despite the simplifications introduced into the analysis, particularly with respect to the assumption of uniform variation of soil stiffness with depth, the model has shown a close agreement against the measured wall deflections and certainly within a range that is acceptable for design purposes.

2. *Cantilevered contiguous pile wall in Lias Clay*

A retaining wall formed from 1500 mm diameter contiguous bored piles has been constructed to support a basement excavation of up to 11.3 m depth in over-consolidated

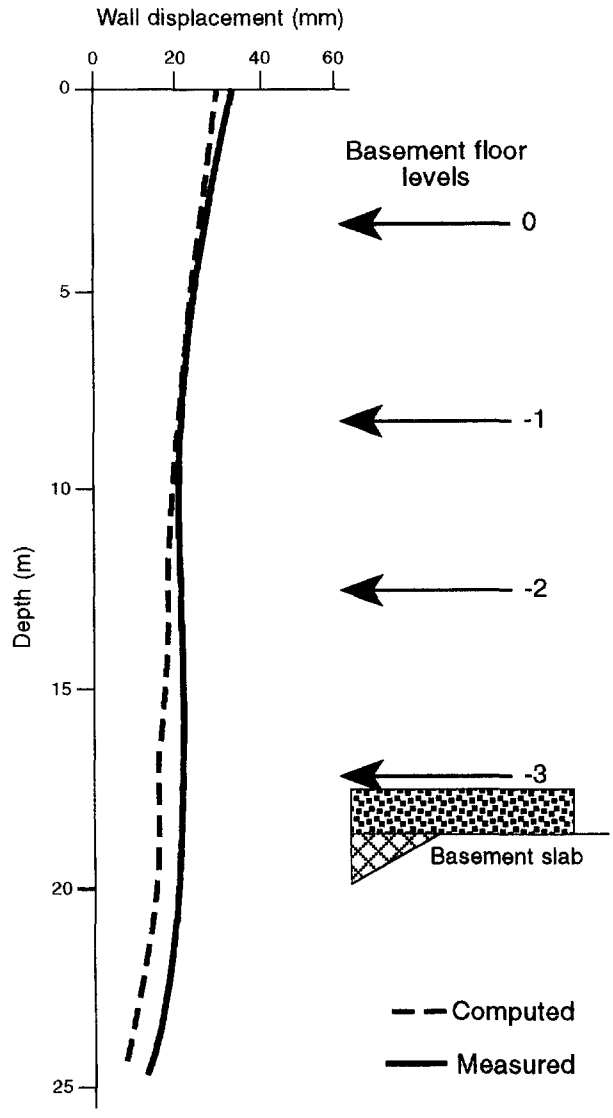

Fig. 9. Measured and computed displacements of main wall at Victoria Embankment.

Lias Clay in Gloucestershire, UK. The wall was constructed as a free cantilever during construction, with the wall being propped by the basement raft in the long term. Construction and monitoring details of this project are provided in Ford *et al.* (1991). Since during construction the wall acted as a free cantilever, a berm of soil was left against the wall and then removed in small sections to install the foundation raft (this measure results in an increase in stability and a reduction in wall displacement).

The ground profile at the site comprises typically 0.7 m of topsoil and locally derived clayey fill material overlying weathered Lias Clay as shown in Fig. 10. About 4 m below ground level this grades into relatively unweathered Lias Clay which extends to depth. The weathered Lias Clay is generally a soft to firm silty clay which becomes firm or stiff and fissured with depth. The unweathered Lias Clay is typically a stiff, fissured silty clay which becomes harder with depth. Three fossiliferous bands were identified in the Lias Clay; the principal one, being 1 to 2 m thick, lies about 4 m below the underside of the foundation raft (see Fig. 10). The standard penetration test (SPT) blowcounts, N, along with the measured undrained shear strength values are shown in Fig. 11. The measured undrained strengths were adjusted using Ladd *et al.*'s (1977) correction to take account of the predominantly horizontal direction in which the soil would be stressed as a result of wall movements. The undrained shear strength profile adopted for numerical analysis is shown

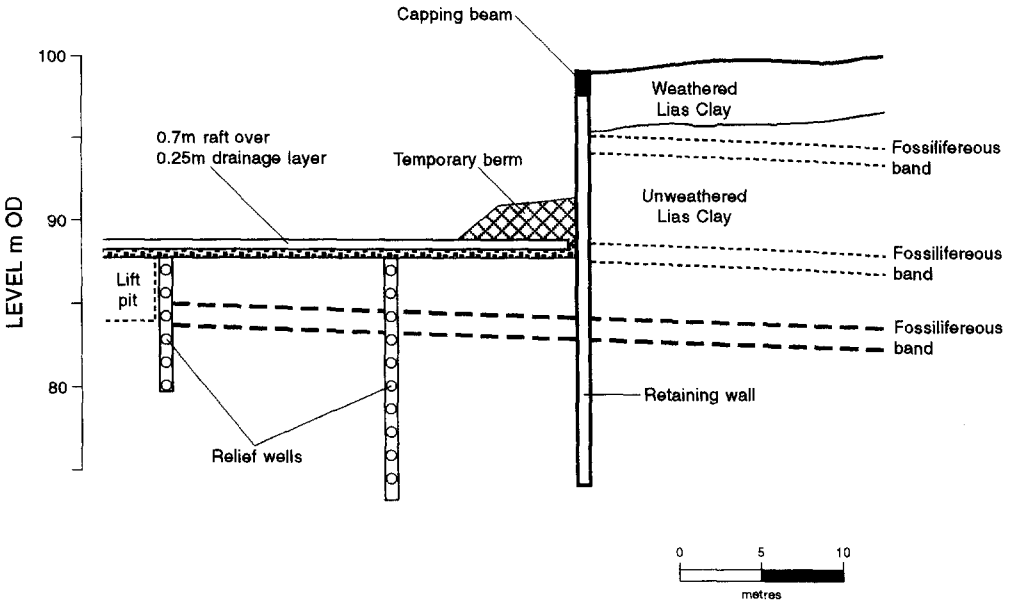

Fig. 10. Cross section of the site geology and construction details (Ford *et al.*, 1991).

in Fig. 11 as the design line. For the soil it is assumed that $E \approx 500\ c_u$; this is consistent with the findings of Cole and Burland (1972), St John (1975), and Burland *et al.* (1979) based on back analyses of deep excavations in London Clay.

Groundwater table was encountered at 1.3 m below ground surface. Groundwater seepages observed during wall installation were associated with the fossiliferous bands which also provided underdrainage within the Lias Clay. The pneumatic piezometers installed within the construction site indicated that the Lias Clay responded essentially in an undrained manner through the excavation phase. Standpipes installed in the pressure relief wells throughout the excavation showed that the water levels within these wells equilibrated within a few days of either carrying out the excavation work or implementing changes to the pumping regime required within the excavation. This pumping was primarily from the lift pits which intersected the principal fossiliferous layer (Fig. 10).

To determine the initial stress conditions self boring pressuremeter tests were performed. Two problems, however, were encountered. First, the pressuremeter device was unable to penetrate more than 6 m into the Lias Clay and second, the results obtained were extremely variable. *In situ* stresses prior to wall construction were therefore assessed using the following empirical relationship as proposed by Mesri and Hayat (1993):

$$K_0 = (1 - \sin\phi')OCR^{\sin\phi_{cv}} \tag{20}$$

where ϕ_{cv} is the constant volume friction angle and OCR is the over-consolidation ratio which can be calculated using the empirical relationship proposed by Mayne (1988):

$$OCR = \left[\frac{c_u/\sigma'_{v0}}{0.75\sin\phi'}\right]^{1.43}. \tag{21}$$

In the above, the design line c_u shown in Fig. 11 was used; ϕ' of 25°–28° and ϕ_{cv} of 22°–25° were used depending on the soil plasticity, and σ'_{v0} (the initial effective vertical stress) was estimated on the basis of a hydrostatic pore water distribution below the groundwater table and soil bulk density within a range between 17 and 19 kN/m^3. The K_0 obtained in this manner was reduced to account for stress relief caused by the wall installation. The adjusted variation of K_0 with depth, as used in the analysis, is shown in Fig. 12.

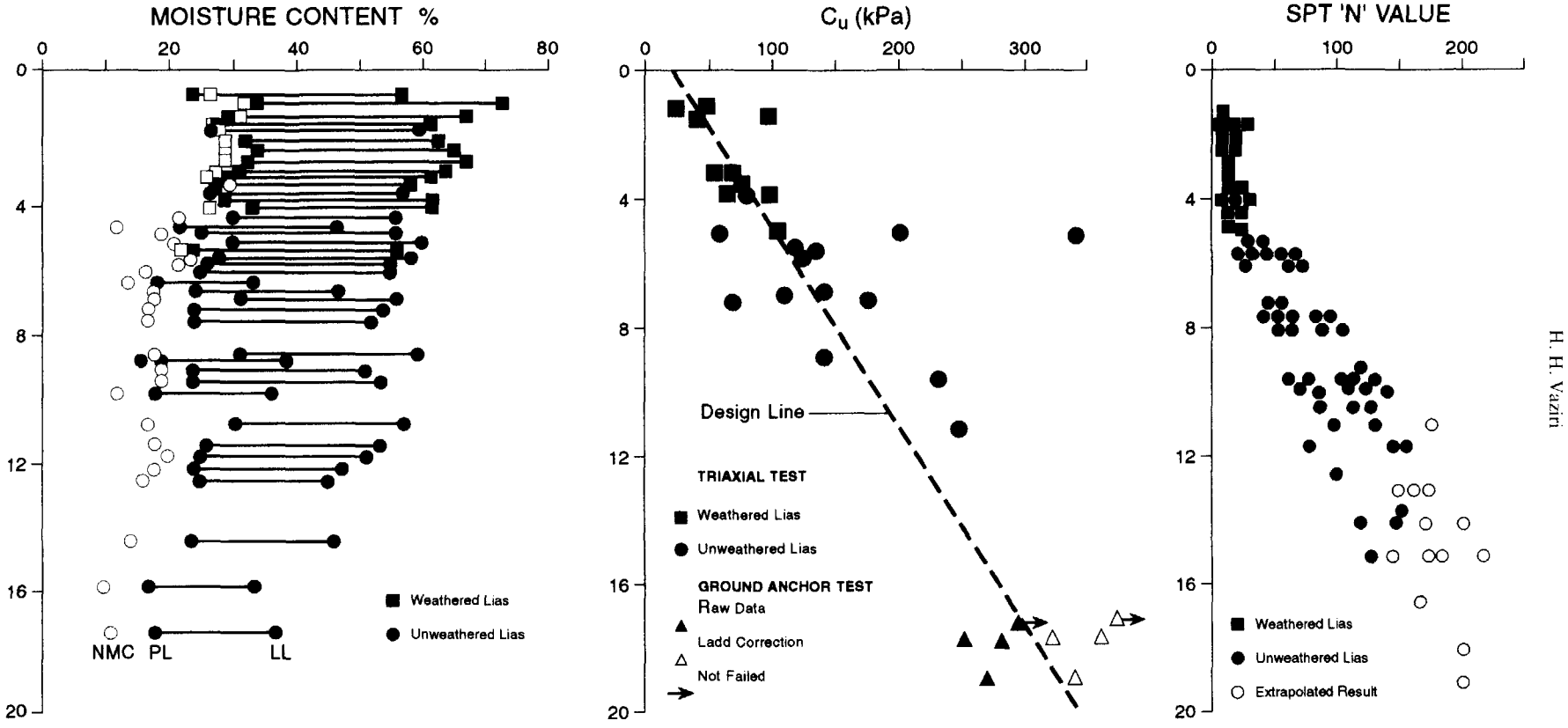

Fig. 11. Measured and inferred soil characteristics.

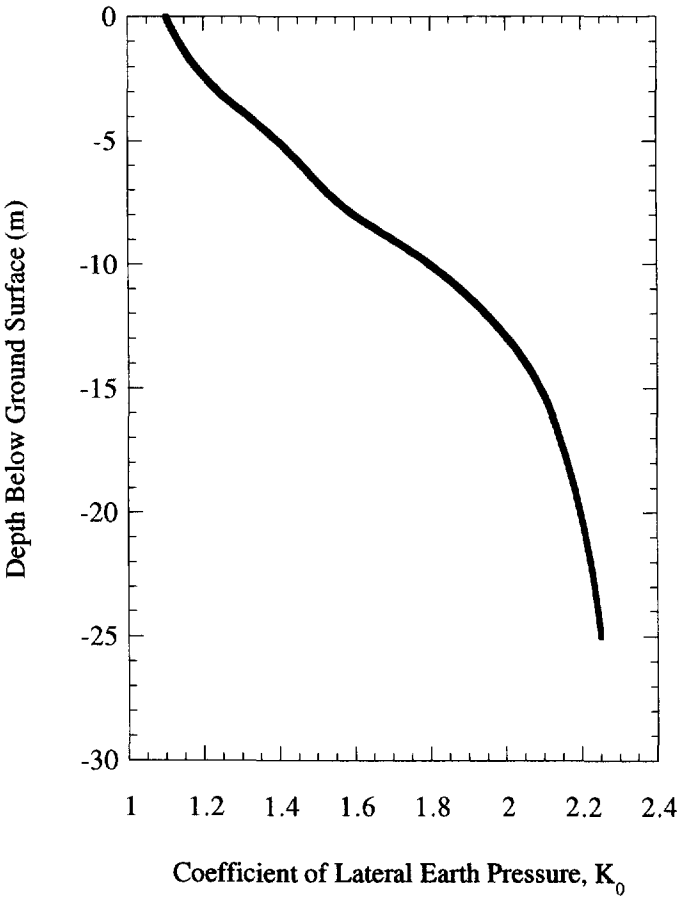

Fig. 12. Variation of K_0 with depth with due allowance for wall installation, Gloucestershire.

The numerical simulation was performed assuming undrained conditions. For the wall, $EI = 2.1$ GN/m^2 was used. For the soil the following strength and stiffness numbers were used

$$c_u = 20 + 16Z \quad \text{(kPa)} \tag{22}$$

$$E_u = 10 + 8Z \quad \text{(MPa)} \tag{23}$$

where Z is the depth below ground surface in meters.

Comparison of the measured and computed wall movements at two different stages corresponding to (a) before removal of the berm, and (b) after raft completion is shown in Fig. 13. For stage (a) corresponding to placement of a berm at the end of excavation, numerical simulation was performed by applying a strut that provides an equivalent resistance as that of the berm. The stiffness of the strut was adjusted to provide a reasonable match against the measured deflection in the vicinity of the berm. The wall deflection at the completion of construction is somewhat larger than the measured deflection. One reason for this is that in the field the berm was removed in small bays as the raft was being constructed; the excavation in small lengths in this final stage of excavation will render smaller displacements as compared to the numerical simulation which assumes a plane strain excavation. The influence of excavation in small lengths on displacements is discussed in Vaziri and Troughton (1992).

3. *Anchored steel soldier piles in soft soils*

This project involves construction of a deep basement to provide 5 levels of parking space beneath a 13-storey office complex in central Johannesburg. The excavation area was

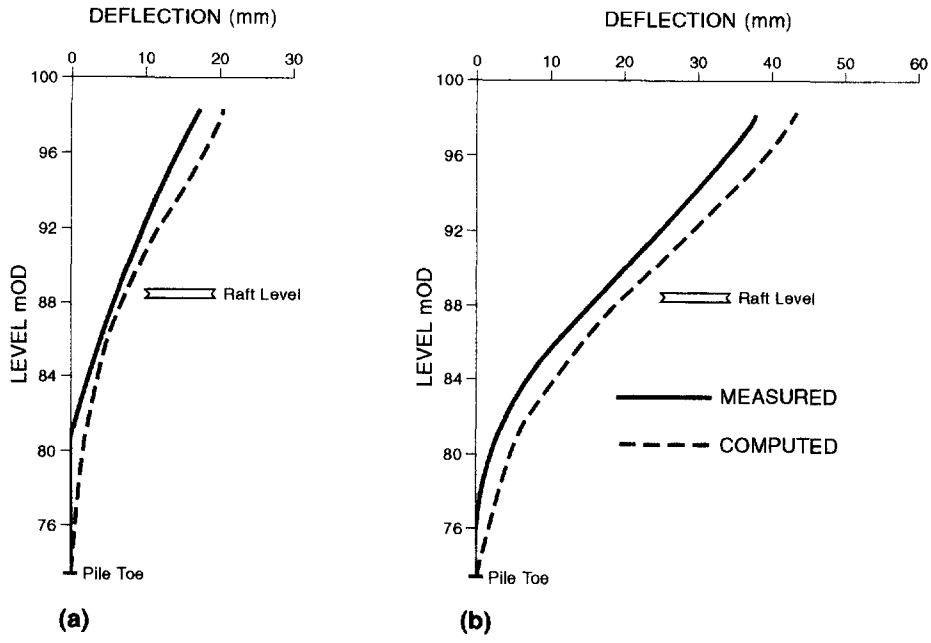

Fig. 13. Comparison of computed and measured movements at (a) end of general excavation with berm and (b) immediately after raft completion.

47.2 m long by 31.4 m wide and about 20 m deep; at one side the excavation face was almost flush against the boundary of an existing 10-storey structure. The latter was founded on 12 m long driven cast-*in situ* piles as schematically shown in Fig. 14 (Day, 1994). In view of the sensitivity of the adjacent buildings, roads and services to movements, the use of continuous soldier piles was favoured against hand-over-hand installation of short lengths of soldiers. On the side of the adjacent existing building (west side) driven replacement cast-*in situ* piles were adopted which were also used to form part of the underpinning system. The piles along the remaining faces comprised steel sections encased in a weak sand cement extending to a depth of 24 m. The steel soldiers comprised two 356 × 171 × 51 kg/m beam sections encased in a weak grout.

All anchors installed on the site were re-injectable anchors with a 6-m fixed length. Installation involved drilling a 75-mm diameter hole inclined at 5° to the horizontal on the west side (to limit the vertical load component of the piles) and 15° elsewhere. On the west side the anchors were positioned between the existing piles as far as possible. The anchor holes were filled with a low viscosity cement grout and the anchors were homed into this

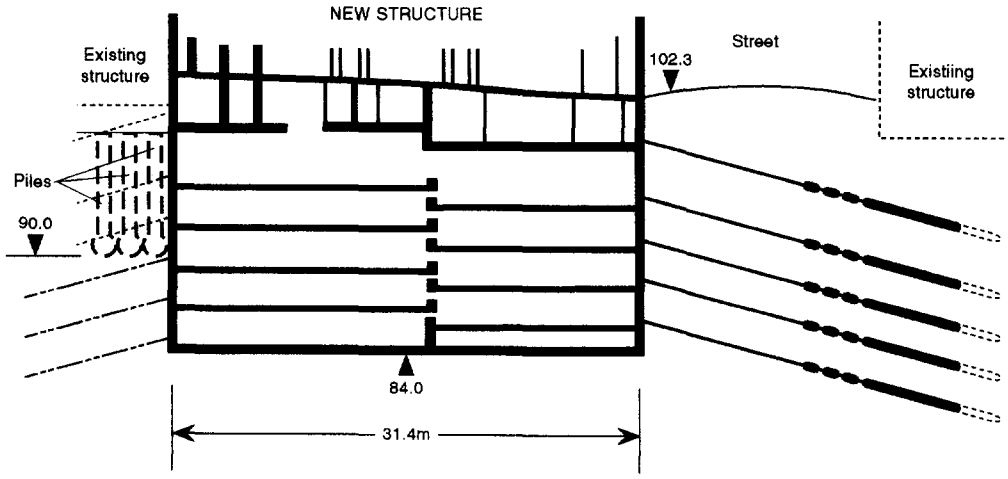

Fig. 14. Section through proposed five basement levels (Day, 1994).

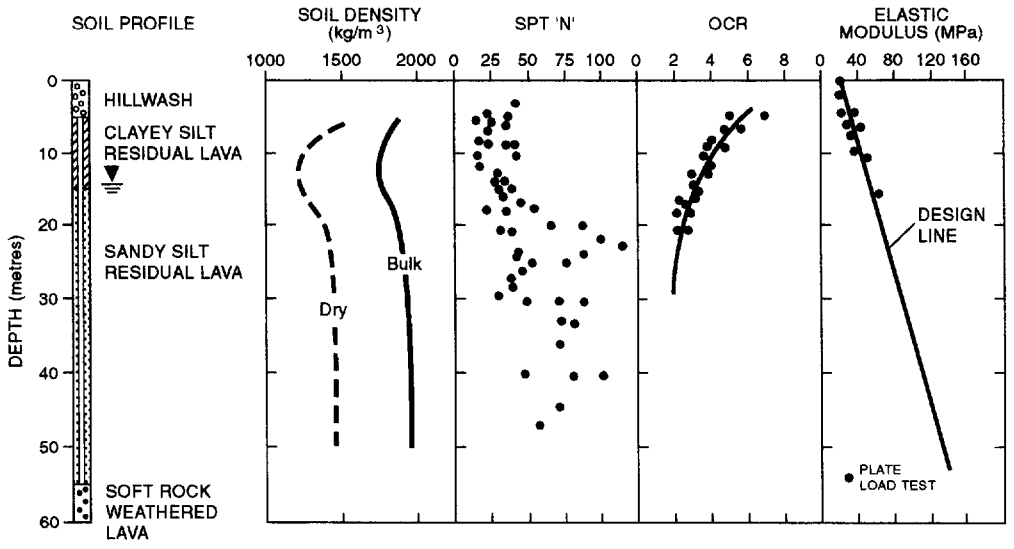

Fig. 15. Measured and inferred soil properties.

grout. Each anchor was stressed incrementally to 750 kN and then rebounded. After two loading/unloading cycles the anchors were locked off at 660 kN.

Typical soil properties at the site are shown in Fig. 15 (Day, 1994). The soil profile indicates a water table at approximately 13 m below the surface. The effective shear strength properties of the residual lava were determined by means of slow, undrained triaxial tests with pore pressure measurements and drained shear box tests. The measured average strength parameters were $c' = 38$ kPa and $\phi' = 29°$. These measurements were obtained by testing intact specimens whereas the soil mass contained numerous relict joints. As those joints were clean and free of clayey infillings, their effect was to reduce cohesion while leaving the angle of friction unaltered. The cohesion assumed for design was therefore reduced; the adopted design parameters are shown in Table 2.

In order to account for the stresses carried by the friction piles beneath the adjacent building on the west side, it was assumed that on the active side the unit weight of the soil within a depth of 12 m has been increased to 35 kN/m^3.

To establish the initial stress conditions the OCR values shown in Fig. 15 were used in conjunction with the relationship shown in eqn (20) to yield the K_0 variation shown in Fig. 16. As explained earlier, the adjustment made to K_0 values is with respect to the inevitable reduction in lateral stress that accompanies the wall installation.

With reference to Fig. 15, the elastic modulus was assumed to vary in accordance with eqn (24) and the Poisson's ratio was chosen as 0.2 throughout.

$$E' = 20 + 3Z \quad \text{(MPa)} \tag{24}$$

The numerical analysis was performed for the excavation on the west side which was the most critical section. The excavation was simulated in several stages as shown in Fig. 17. Each stage involved excavation followed by placement of a strut and a further excavation. The struts were placed at depths of 3.2, 7.4, 10.4, 14.2 and 17.5 m below the surface.

Table 2. Design parameters to characterize the soil response

Soil type	Consistency	Thickness (m)	γ_{bulk} (kN/m^3)	ϕ'	ϕ_{cv}	c' (kPa)	K_a	K_P
Hillwash (gravel, sand and clay)	Medium dense to dense	5.0	17.5	35°	30°	0.0	0.27	3.70
Andesite (clayey silt)	Firm	15.0	18.5	29°	25°	10	0.35	2.88

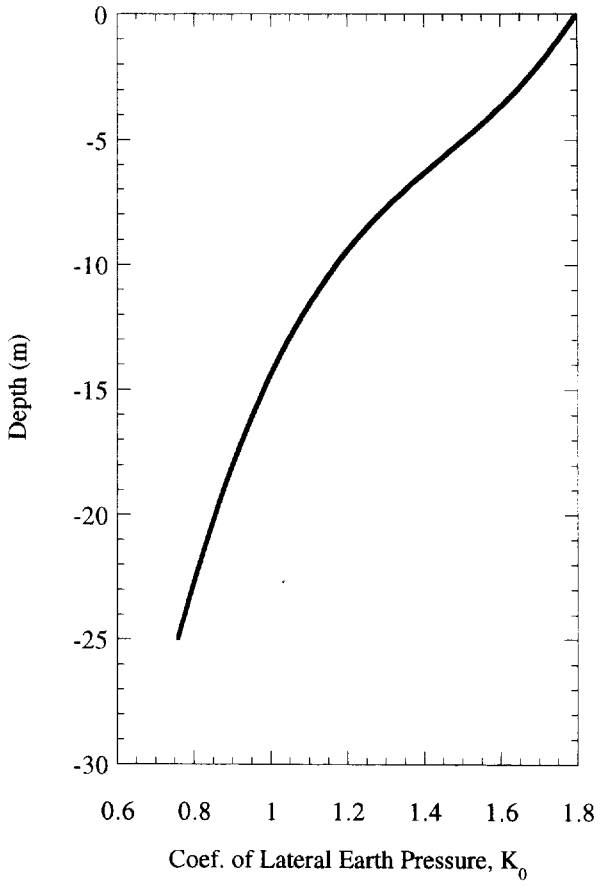

Fig. 16. Variation of K_0 with depth with due allowance for wall installation, Johannensburg.

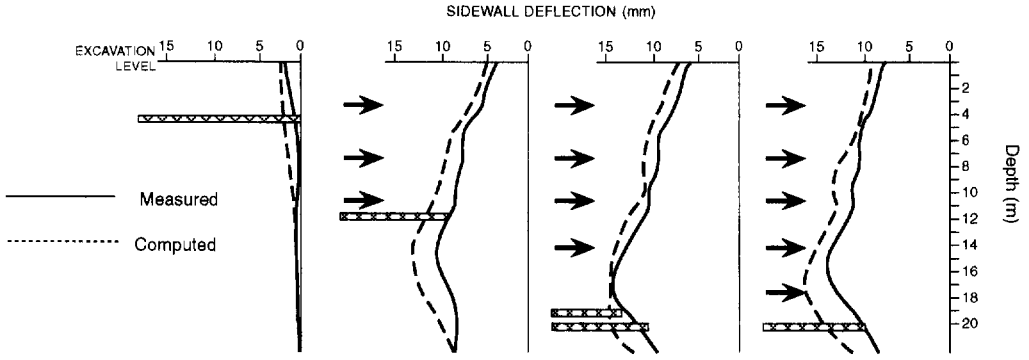

Fig. 17. Computed and measured wall deflection on the west side at different stages of construction.

Comparison of the measured and computed wall deflections show a reasonably good agreement at different stages of construction.

SUMMARY AND CONCLUSIONS

A simple numerical model is described for analysis of strutted flexible retaining walls. The model can perform stability analysis and compute deformation, bending moment and shear force in the wall and forces in any struts resulting from excavation, changes in water pressure or application of surcharge. The model has direct application in constructions involving driven sheetpiles, bored reinforced concrete piles or trench excavated concrete diaphragm walls.

The methodology used to model the the stiffness response of the soil mass involves representing the soil to each side of the wall by an elastic solid, the flexibility of which is generated by interpolation and sealing of flexibility matrices calculated for a simplified soil model using finite element methods. A semi-empirical formulation has been used to allow for variations in the soil stiffness with depth. The wall stiffness is represented by a series of elastic beam elements. In addition the earth pressures are limited to be within active and passive limits. Other features that can be accommodated by the program include struts, anchors, variations in water table and the effects of surcharges.

In back analysis of several field problems, it has been shown that the model can capture both the mode and magnitude of wall displacements reasonably well. In performing these analyses which included a wide range of parametric studies the following points were observed:

—the stiffness modulus derived from back-analysis of field measurements tends to be several times larger than that obtained from the conventional laboratory tests. The main reason for this discrepancy can be linked to the strain levels that are much higher in laboratory tests than would occur in the field under working stress conditions;
—the behaviour of an earth retaining structure is likely to be influenced by details of construction procedure, such as the method used to form the wall, the rigidity of any support system and the sequence of excavation;
—the properties of the wall, characterized by its EI, seem to play a smaller role in controlling movements than its physical appearance might suggest. Other attributes of the wall, such as height and depth of penetration have a greater influence on the wall movements;
—most movement takes place below the level of the lowest support at any stage, therefore, the greatest benefit is gained if supports are inserted quickly and at small intervals. Once a support is inserted, provided it is reasonably rigid, little subsequent movement takes place and the effective stiffness of the support is not very important;
—variations in soil parameters K_0 and ν within a range that can be reasonably defined using conventional soil data, do not appreciably influence wall deflections.

In practice, one of the greatest benefits to draw from the proposed model is in its use as an efficient design tool for performing sensitivity analysis (such as in quantifying the influence of strutting sequence) and in attaining a better understanding of the mechanisms of behaviour of the ground and structure and the likely magnitudes and extent of ground movements. Moreover, as demonstrated in the cases analysed herein, the model can also be used quite effectively for predicting the wall performance under field conditions.

Acknowledgements—Much of the fundamental work on the work reported here was completed during 1979 to 1981 while the author was employed as a geotechnical engineer at Ove Arup and Partners in London, UK. My colleagues, Dr J. W. Pappin and Dr B. Simpson, provided many of the ideas used in this paper and their significant contributions are gratefully acknowledged. The corrections made and several insightful suggestions provided by the anonymous reviewer of this paper have been highly instrumental in improving the accuracy and usefulness of the final product.

REFERENCES

Burland, J. B. and Hancock, R. J. R. (1977). Underground car park at the House of Commons, London: geotechnical aspects. *The Structural Engineer* **55**, 87–100.

Burland, J. B., Simpson, B. and St John, H. D. (1979). Movements around excavations in London Clay. In *Design Parameters in Geotechnical Engineering, Proc. 7th Eur. Conf. Soil Mech., Brighton*, Vol. 1, pp. 13–30.

Cole, K. W. and Burland, J. B. (1972). Observations of retaining wall movements associated with a large excavation. In *Proc. 5th Eur. Conf. Soil Mech. Fdn Engng, Madrid*, Vol. 1, pp. 445–453.

Day, P. 1994. Design and construction of deep basement in soft residual soils. In *Proc. ASCE National Convention*, Atlanta, GA, Publication No. 942, 734–746.

Ford, C. J., Chandler, C. J. and Chartres, F. R. D. (1991). The monitoring and back analysis of a large retaining wall in Lias Clay. In *Proc. 10th European Conf. on Soil Mechanics and Foundation Engng*, Florence, pp. 707–710.

Jardine, R. J., Potts, D. M., St. John, H. D. and Hight, D. W. (1991). Some practical applications of a non-linear ground model. In *Proc. 10th European Conf. on Soil Mechanics and Foundation Engng*, Florence, pp. 223–228.

Ladd, C. C., Foott, R., Ishihara, K., Schloser, F. and Poulos, H. G. (1977). Stress-deformation and strength characteristics. *State-of-the-art report. Proc. 9th ICSMFE*, Tokyo, Vol. 2, pp. 421–494.

Mair, R. J. 1993. Developments in geotechnical engineering research : application to tunnels and deep excavations. In *Proc. Instn Civ. Engrs and Civ. Engng*, Paper 10070, 93, Feb., pp. 27–41.

Mayne, P. W. (1988). Determining OCR in calys from laboratory strength. *ASCE J. Geot. Engng*, **114,** 76–92.

Mesri, G. and Hayat, T. M. (1993). The coefficient of earth pressure at rest. *Canadian Geotechnical J.* **30,** 647–666.

Pappin, J. W., Simpson, B., Felton, P. J. and Raison, C. (1985). Numerical analysis of flexible retaining walls. In *Proc. Conf. Num. Methods in Eng. Theory and Applications*, Swansea.

St John, H. D. (1975). Field and theoretical studies of the behaviour of ground around deep excavations in London clay. Ph.D. thesis, University of Cambridge.

St John, H. D., Potts, D. M., Jardine, R. J. and Higgins, K. G. (1993). Prediction and performance of ground response due to construction of a deep basement at 60 Victoria Embankment. In *Proc. Wroth Memorial Symposium*, Oxford.

Vaziri, H., Simpson, B., Pappin, J. W., & Simpson, L. (1982). Integrated forms of Mindlin's equations. *Geotechnique* **32,** 275–277.

Vaziri, H. H. and Troughton, V. (1992). An efficient three-dimensional soil-structure interaction model. *Can. Geot. J.* **29,** 529–538.

Vaziri, H. H. 1995. Theory and application of an efficient computer program for analysis of flexible earth-retaining structures. *Comput. Struct.* **56,** 177–187.

Whittle, A. J., Hashash, Y. M. A. and Whitman, R. V. (1993). Analysis of deep excavation in Boston. *J. Geotech. Engng., ASCE* **119,** 69–90.